The Structure and Characterization of a Modular Endo-β-1,4-mannanase from *Cellulomonas fimi*[†,‡]

Jérôme Le Nours,[§] Lars Anderson,[||] Dominik Stoll,[⊥] Henrik Stålbrand,[||] and Leila Lo Leggio*[,§]

Centre for Crystallographic Studies, Biophysical Chemistry Group, Department of Chemistry, University of Copenhagen, Universitetsparken 5, DK-2100 Copenhagen, Denmark, Department of Biochemistry, Lund University, P.O. Box 124, SE-221 00 Lund, Sweden, and Department of Microbiology and Immunology, University of British Columbia, 300-6174 University Boulevard, Vancouver, British Columbia, Canada V6T 1Z3

Received April 28, 2005; Revised Manuscript Received July 16, 2005

ABSTRACT: The endo-β-1,4-mannanase from the soil bacterium *Cellulomonas fimi* is a modular plant cell wall degrading enzyme involved in the hydrolysis of the backbone of mannan, one of the most abundant polysaccharides of the hemicellulosic network in the plant cell wall. The crystal structure of a recombinant truncated endo-β-1,4-mannanase from *C. fimi* (CfMan26A-50K) was determined by X-ray crystallography to 2.25 Å resolution using the molecular replacement technique. The overall structure of the enzyme consists of a core $(\beta/\alpha)_8$-barrel catalytic module characteristic of clan GH-A, connected via a linker to an immunoglobulin-like module of unknown function. A complex with the oligosaccharide mannotriose to 2.9 Å resolution has also been obtained. Both the native structure and the complex show a cacodylate ion bound at the −1 subsite, while subsites −2, −3, and −4 are occupied by mannotriose in the complex. Enzyme kinetic analysis and the analysis of hydrolysis products from manno-oligosaccharides and mannopentitol suggest five important active-site cleft subsites. CfMan26A-50K has a high affinity −3 subsite with Phe325 as an aromatic platform, which explains the mannose releasing property of the enzyme. Structural differences with the homologous *Cellvibrio japonicus* β-1,4-mannanase (CjMan26A) at the −2 and −3 subsites may explain the poor performance of CfMan26A mutants as "glycosynthases".

The plant cell wall is a very complex network of polysaccharides. Hemicellulose is the second most abundant constituent (about 20%−30%) of the network. It is composed of an assembly of a variety of monosaccharides including xylose, arabinose, and mannose. The major soft-wood hemicellulose is acetylated galactoglucomannan, which has a backbone composed of β-1,4-linked D-mannopyranosyl and D-glucopyranosyl residues (*1*, *2*). It carries acetyl- and galactosyl substitutions. Other types of mannans function in seeds as storage polysaccharides. Endo-β-1,4-mannanases (EC 3.2.1.78) are retaining glycoside hydrolases (*3*) which are involved in the enzymatic degradation of the β-1,4-*O*-mannosidic bonds in mannan and heteromannans such as galactomannan, glucomannan, and galactoglucomannan. β-1,4-Mannanases have mostly been assigned to family 5 and family 26 of the glycoside hydrolases, both belonging to clan GH-A[1] (*4*, *5*). Structures of two β-1,4-mannanases from family 5 in complex with oligosaccharide products have been determined by X-ray crystallography (*6*, *7*). Recently, the structure of a family 5 tomato β-1,4-mannanase (*8*) and the preliminary structure determination of a bacterial family 5 β-1,4-mannanase (*9*) have been reported. Not as much information is available for family 26 (GH-26) mannanases, where only one member of the family has been structurally characterized. Almost a decade ago, the first biochemical investigations were performed on the family 26 β-1,4-mannanase A from *Cellvibrio japonicus* (formerly *Pseudomonas cellulosa*) which led to the identification of amino acid residues Glu212 and Glu320 as catalytic residues (*10*). A few years later, the three-dimensional structure was determined to 1.85 Å by Hogg et al. (*11*) and was the first, and so far the only, structure of an enzyme belonging to glycoside hydrolase family 26. As expected for a clan GH-A member, the *C. japonicus* β-1,4-mannanase (CjMan26A) structure exhibited the $(\beta/\alpha)_8$-barrel overall architecture and the catalytic nucleophile and acid/base residues were located at the end of the β-strands 4 and 7, respectively. Further structural investigations to high resolution of the CjMan26A catalytic mutant Glu212Ala suggested that the mannopyranosyl moiety bound at the −1 subsite will adopt an unusual $B_{2,5}$ conformation for the transition state (*12*). According to

[†] This research was supported by The Danish National Research Foundation (DGF), the Danish Natural Science Research Council (SNF), and the Swedish Research Council (VR).

[‡] The structures described in this article have been deposited with the Protein Data Bank with codes 2BVY and 2BVT.

* To whom correspondence should be addressed. Phone: +45 35320295. Fax: +45 353 20322. E-mail: leila@ccs.ki.ku.dk.

[§] University of Copenhagen.

[||] Lund University.

[⊥] University of British Columbia.

[1] Abbreviations: BSA, bovine serum albumin; CBM, carbohydrate binding module; Clan GH-A, glycoside hydrolases-clan A; CjMan26A, the β-1,4-mannanase from *Cellvibrio japonicus*; CfMan26A, the full-length β-1,4-mannanase from *Cellulomonas fimi*; CfMan26A-50K, the amino terminal 50kDa stable fragment of the β-1,4-mannanase from *C. fimi*; GH-26, glycoside hydrolase family 26; Ig-like, immunoglobulin-like; IPTG, isopropyl-β-D-thio-galactopyranoside; M1, mannose; M2, mannobiose; M3, mannotriose; M4, mannotetraose; M5, mannopentaose; M6, mannohexaose; SCOP, structural classification of proteins; SLH, S-layer homology; TrMan5A, the *Trichoderma reesei* β-1,4-mannanase 5A; AnMan5A, the *Aspergillus niger* β-1,4-mannanase.

10.1021/bi050779v CCC: $30.25
Published on Web 08/27/2005

the commonly used nomenclature, subsites −1 and +1 are occupied by the monomers adjacent to the hydrolyzed glycosidic bond, with the reducing end of the substrate on the + side.

Frequently, β-1,4-mannanases (*13*, *14*) and other polysaccharidases carry extra modules besides the catalytic module (*15*). The most common ones are the carbohydrate-binding modules (CBMs) (*16*), which have been classified in at least 36 families (*17*). The modules are usually connected by linker regions with a typical length of about 10−30 residues. Stoll et al. (*18*) previously identified and described a β-1,4-mannanase from *Cellulomonas fimi* which displays an unusual modular architecture and consists of 951 amino acid residues. This work showed that the mature enzyme contained at least a catalytic module from GH-26, a putative SLH module, and two modules of unknown function. One of the latter modules was later characterized as a mannan-binding module (*19*) and was classified as the family 23 of CBMs. Proteolysis of the mature β-1,4-mannanase (*18*) by a *C. fimi* secreted protease led to the release of a large and stable fragment corresponding to about 460 residues and comprising the catalytic domain and 50 to 60 extra residues at the C-terminus. A 50 kDa recombinant variant of the fragment (named CfMan26A-50K) was studied in this work. The study describes the three-dimensional structure and functional analysis of CfMan26A-50K.

EXPERIMENTAL PROCEDURES

Enzyme Expression and Purification. CfMan26A-50K (amino acids 1 to 464 of CfMan26A) attributed with a carboxy terminal $(His)_6$-affinity tag was recombinantly expressed by *Escherichia coli* cells transformed with a pET28b plasmid (Novagen, Madison, WI) carrying the appropriate insert. The protein was purified essentially as described previously for CfMan26A (*18*). An overnight culture was diluted in 200 mL of Luria broth containing 50 μg/mL kanamycin and was grown at 37 °C until OD_{600} reached 1.3. Induction of CfMan26A-50K expression was started by adding 0.4 mM IPTG. Cells were then grown at 15 °C for 24 h followed by harvesting by centrifugation (SLA-3000, 5000 rpm). The cells were ruptured three times using a French pressure cell, and a centrifugation step was performed to remove debris and unbroken cells. The supernatant was equilibrated in binding buffer (5 mM imidazole, 500 mM NaCl, 20 mM tris-HCl, pH 7.9) and was loaded on a 5 mL HisBind column (Novagen, Madison, WI). Elution was performed by a stepwise increase of imidazole (5−500 mM), and fractions of 2.5 mL were collected. Fractions were tested for β-mannanase activity using the dinitrosalicylic assay (*20*). CfMan26A-50K appeared as a single band of 50 kDa on SDS−PAGE after silver staining. The purified protein was concentrated using a MicroSep 10 kDa cutoff spin-column (Pall, East Hills, NY), and the buffer was exchanged by concentrating and diluting the sample three times with 50 mM Na-citrate buffer (pH 6.0). The purified protein was adjusted to an estimated final concentration of 10 mg/mL.

Crystallization. An enzyme concentration of 10 mg/mL was used in the subsequent crystallization trials, which were all carried out by the hanging-drop vapor diffusion method at room temperature. A solubility screen (*21*) consisting of a drop composed of 2 μL of reservoir solution and 2 μL of protein was first set up. After 24 h, crystals presenting three distinct morphologies were formed with the crystallization conditions composed of either 1.6 or 2 M phosphate, pH 7, and also with conditions composed of either 1.5 or 2 M ammonium sulfate, pH 7. These three crystal forms were tested using synchrotron sources at beamline I711 (MaxLab, Lund, Sweden) (*22*), DESY (Hamburg-Germany), and ID-29 (ESRF, Grenoble, France) and diffracted to about 3.0−4.0 Å resolution. Further crystallization conditions were screened using the Hampton crystal screen I (*23*), and crystals grew under numerous conditions, using either salts or PEG as main precipitants. With PEG as the main precipitant, conditions producing crystals contained sodium cacodylate as buffer as in (i) 18% w/v PEG 8000, 0.1 M sodium cacodylate pH 6.5, 0.2 M calcium acetate, (ii) 20% w/v PEG 8000, 0.1 M sodium cacodylate pH 6.5, 0.2 M magnesium acetate trihydrate, and (iii) 30% w/v PEG 8000, 0.1 M sodium cacodylate pH 6.5, 0.2 M sodium acetate trihydrate. A crystal obtained from condition (iii) turned out to be of a suitable quality for structure determination of the enzyme.

Data Collection and Processing. A CfMan26A-50K crystal was soaked in mother liquor containing 30% (v/v) glycerol prior to flash cooling in liquid nitrogen. X-ray data were collected at beamline ID-23-1 at ESRF (Grenoble-France) and were processed using *HKL2000* (*24*). The space group was determined to be $P2_12_12_1$ with one molecule in the asymmetric unit. Crystals grown under similar conditions were soaked in mother liquor solution cryoprotected with 30% glycerol and containing 0.3 M mannotriose. Data were collected at beamline I711, MAXLAB, Lund, Sweden and processed with HKL 1.96.1 (*24*). The space group was also $P2_12_12_1$, but the crystals were not isomorphous and contained two molecules in the asymmetric unit. The data collection statistics are listed in Table 1. The relatively low completeness of the data for the mannotriose complex is due to high mosaicity (1.5° as refined by Scalepack) leading to overlapping reflections.

Structure Determination and Refinement. The structure of CfMan26A-50K was determined by the molecular replacement method with the program MOLREP (*25*). The native CjMan26A structure determined to 1.85 Å (PDB code: 1j9y) (*11*) and sharing about 40% sequence identity with the *C. fimi* enzyme was used as search model. At this stage, data from 30 to 3.5 Å resolution were used. A clear solution was identified and gave a correlation coefficient of 46.3% and an *R*-factor of 54.7%. 10% of the observed reflections were randomly removed for cross-validation (*26*), and a rigid-body refinement of the correct solution was then performed in CNS (*27*). The data from 30 to 2.25 Å resolution were used for the rest of the refinement. Based on the sequence alignment of the *C. fimi* and *C. japonicus* β-1,4-mannanases, the mutations from the model to target sequence and the successive manual rebuilding were conducted with the program *O* (*28*) including removal of loops not expected in CfMan26A-50K and building of those not present in CjMan26A. Each step of the manual rebuilding was followed by slow-cool simulated annealing minimization and *B*-factor refinement using the program CNS. The $F_o - F_c$ electron density map showed clear density in the active site for a cacodylate ion which originated from the crystallization mixture. This molecule was therefore included in the model. The crystallized CfMan26A-50K contained about 100 extra

Table 1: Data Collection and Refinement Statistics

parameters	CfMan26A-50K	mannotriose complex
temperature (K)	100	100
space group	$P2_12_12_1$	$P2_12_12_1$
a, *b*, *c* (Å)	74.25, 82.0, 95.41	73.12, 98.79, 133.13
no. of measd reflns	106 106	93 368
no. of unique reflns	28 207	17 987
resolution range (Å)[a]	50−2.25 (2.33−2.25)	30−2.9 (3.0−2.9)
completeness (%)	98.8 (96.7)	81.7 (66.0)
R_{merge}[b] (%)	6.2 (38.1)	9.9 (31.1)
	Refinement	
R_{work}, R_{free}[c] (%)	19.3, 22.2	20.5, 25.0
non-hydrogen atoms in model		
protein atoms	3386	6772
water molecules	89	10
cacodylate	5	10
glycerol	12	0
acetate	4	0
mannotriose	0	68
rmsd values from ideality		
bond lengths (Å)	0.006	0.007
bond angles (deg)	1.2	1.3
dihedral angles (deg)	24.0	23.7
Ramachandran plot[d] (% residues)		
in most favored regions	91.3	85.2
in allowed regions	8.7	14.8
in generously allowed regions	0	0

[a] Values shown in parentheses correspond to the high-resolution shell. [b] $R_{merge} = \sum_{hkl}\sum_i|I(hkl)_i - \langle I(hkl)\rangle|/\sum_{hkl}\sum_i I(hkl)_i$. [c] $R_{work} = \sum|\{|F_o(hkl)| - k|F_c(hkl)|\}|/\sum|F_o(hkl)|$. R_{free} is calculated for a "test" set of reflections that were not included in the refinement. [d] Calculated by PROCHECK (*47*).

C-terminal amino acid residues relative to the CjMan26A. At the beginning of the refinement, no clear electron density was observed for these extra amino acid residues. The successive refinement cycles of the catalytic module improved significantly the quality of the $F_o - F_c$ electron density map which revealed the presence of these additional amino acid residues forming a new module. A polyalanine model was first built into the electron density and then changed to the correct sequence. This was followed by slow-cool simulated annealing and *B*-factor refinement cycles. At this stage, two glycerol molecules were identified in the active site and inserted into the model. The water molecules were added automatically first and manually to a total of 89. A few successive cycles of positional and *B*-factor refinement were then performed. The final model, consisting of 451 amino acid residues, has a crystallographic *R*-factor of 19.3% and an *R*-free value of 22.2%.

For the mannotriose complex, molecular replacement was carried out in MOLREP using the structure of CfMan26A-50K as a search model. The resulting solution gave a correlation coefficient of 75.7% and an *R*-factor of 33.8%. Refinement was carried out in CNS after insertion of a mannotriose molecule in the active site of each molecule in the asymmetric unit. All the individual mannopyranosyl moieties were inserted in the $^4C_1$ chair conformation. Due to the low resolution (2.9 Å) a constrained NCS protocol was used for refinement. The refinement statistics for the two structures are listed in Table 1.

Analysis of Hydrolysis Products and Enzyme Kinetic Analysis. Mannobiose (M2), mannotriose (M3), mannotetraose (M4), mannopentaose (M5), and mannohexaose (M6) were purchased from Megazyme (Bray, Ireland). Mannose (M1), locust bean gum and guar gum galactomannans were from Sigma (St. Louis, MO). The specific activities on galactomannans were determined at 5 mg/mL substrate concentration with detection of reducing sugars with dinitrosalicylic acid (*20*). The Michaelis−Menten constants of the locust bean gum galactomannan hydrolysis were determined by using 28 nM of enzyme and varying the substrate concentrations (5 mg/mL to 0.313 mg/mL). All hydrolysis experiments were performed at pH 6 using a 50 mM Na-citrate buffer with 0.1 mg/mL bovine serum albumin (BSA) (Sigma) at 37 °C. The reactions were terminated by boiling for 2 min. Hydrolysis of ivory nut mannan (Megazyme, Bray, Ireland) was analyzed by incubating 1 mg/mL ivory nut mannan using 5 μM enzyme for 2 h. For hydrolysis, M2 (10 mM) was incubated with 3 μM enzyme for 48 h. M3 (0.5−10 mM), M4 (0.125−4 mM), M5 (0.125−4 mM), and M6 (0.125−2 mM) were incubated with appropriate concentrations of enzyme (0.46−10 nM). Aliquots were withdrawn at 30, 60, and 90 min. The formed hydrolysis products were analyzed using high performance anion exchange chromatography with pulsed amperometric detection (HPAEC-PAD) with a Dionex CX 500 system (Dionex, Sunnyvale, CA) as described previously (*29*). The hydrolysis product amounts were recalculated to amount of hydrolyzed substrate oligosaccharide. The hydrolysis rate was plotted against substrate concentration, and the kinetic parameters (k_{cat} and K_m) were determined by nonlinear regression using Kaleidagraph 3.51 (Synergy software).

To obtain mannopentitol, 1 mg/mL of M5 was reduced using 200 mM $NaBH_4$ in NaOH (890 mM) for 2 h at room temperature (*30*, *31*). The reaction was neutralized and Na^+ ions were removed by adding Amberlite IR-120(Plus) H^+-form (Sigma). The water and formed boric acid were removed by vacuum centrifugation (40 °C) followed by two washes using 100% methanol and one wash using water. The reduced oligosaccharide was analyzed using HPAEC-PAD. Hydrolysis of mannopentitol was performed at 1 mM substrate concentration using 20 nM enzyme. The incubation was performed at 37 °C in a 50 mM Na-citrate buffer (pH 6) supplemented with 0.1 mg/mL BSA. Samples were withdrawn at regular time points followed by boiling for 2 min. Hydrolysis products were detected using HPAEC-PAD with appropriate standards. Reduced manno-oligosaccharide products were identified by spiking the hydrolysis products with reduced manno-oligosaccharides synthesized as above.

RESULTS AND DISCUSSION

Structure of CfMan26A-50K. The studied protein fragment, CfMan26A-50K, is unexpectedly organized into two modules: a GH-26 catalytic module which is connected via a linker to a second module formed of seven β-strands (Figure 1A). The four first N-terminal amino acid residues (Met, Ala, Asp, and Glu), the last two C-terminal amino acids (Leu468 and Glu469), and the His-tag are not visible in the electron density. The catalytic module consists of residues Met1−Phe354 and exhibits the architecture of the classical $(\beta/\alpha)_8$-barrel folding motif characteristic of a clan-GH-A member. An additional α-helix (Thr14−Arg28) at the N-terminus is also observed. The catalytic acid/base (Glu175) and nucleophile (Glu282) amino acid residues are located at the end β-strands 4 and 7, respectively. The catalytic module is connected via a linker composed of about 20 amino acid

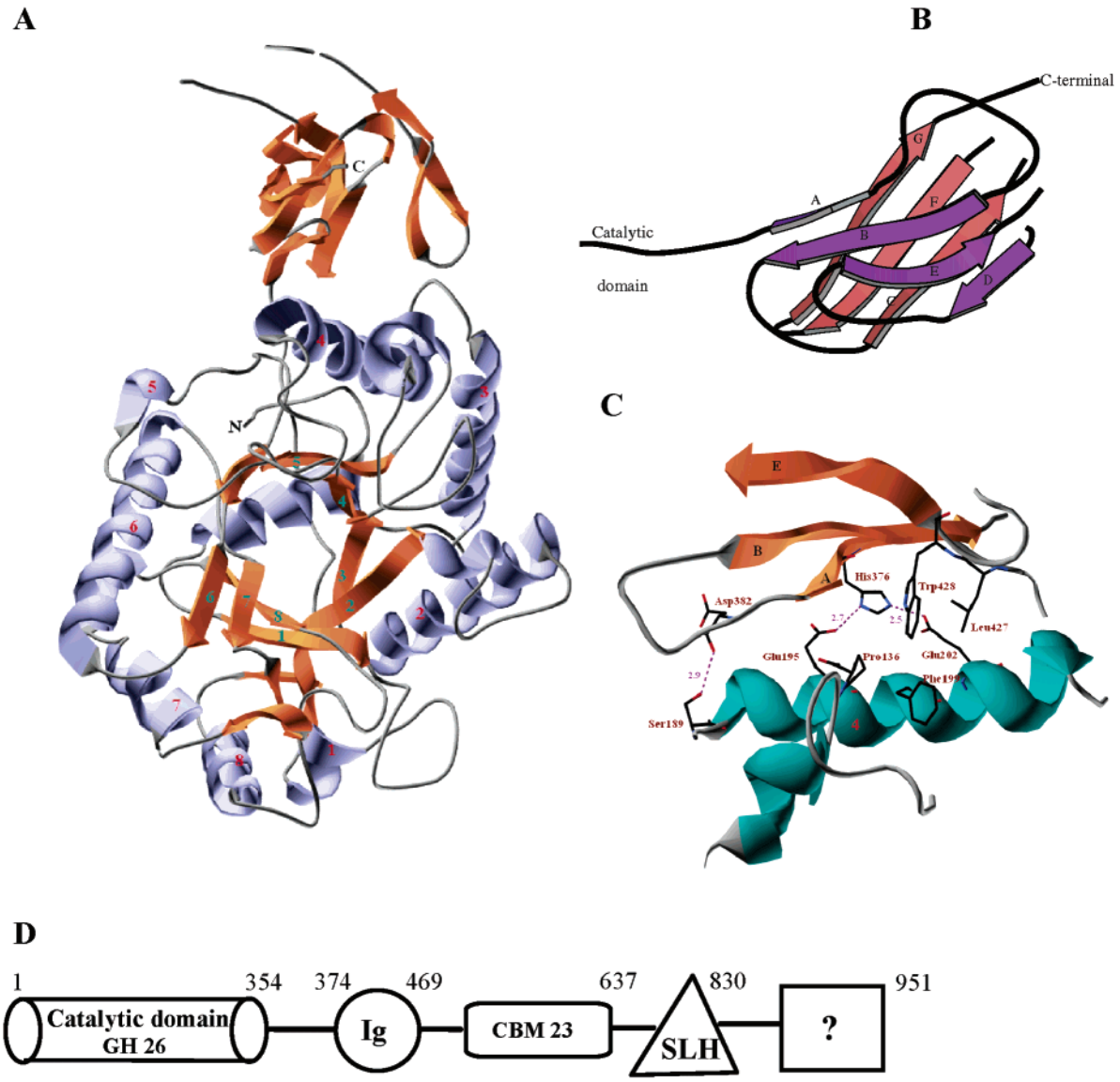

FIGURE 1: (A) Overall fold of the CfMan26A-50K. The α-helices and β-strands belonging to the $(\beta/\alpha)_8$-barrel motif are numbered. (B) Ribbon representation of the β-sheet domain of CfMan26A-50K. (C) Close-up view of the interdomain interface between the catalytic and the β-sheet modules of CfMan26A-50K. (D) Schematic representation of the updated modular architecture of the mature *C. fimi* β-1,4-mannanase. The numbers indicate the positions of the amino acids in the sequence of the mature enzyme. Illustrations A and C were prepared using the program Swiss PDB-viewer (*43*), illustration B was prepared using MOLSCRIPT (*44*), and representation D was prepared using the program Isis/Draw.

residues (from Ala355 to Val374) to the second module consisting of about 90 amino acid residues organized in seven β-strands named A, B, C, D, E, F, and G from the N-terminal to the C-terminal of the module. Linkers between different modules are sometimes not seen in the crystal structures of carbohydrate degrading enzymes. However, in the current case, the linker has several hydrophobic interactions with the catalytic module and has a similar length as the one previously seen in the crystal structure of a bacterial cellulase (*32*). Interactions between the β-sheet module and the catalytic module (Figure 1C) involve mainly hydrogen bonds between amino acid residues belonging to the helix α_4 of the $(\beta/\alpha)_8$-barrel and residues of the β-strand A of the β-sheet module. A hydrophobic interface was also identified and is formed by the amino acid residues Phe199 and Pro136 of the catalytic core and the residues Trp428 and Leu427 of the β-sheet module. These close contacts could fix the relative orientation of the two modules and could be a likely explanation for the proteolytic cleavage occurring after this small β-sheet module. The relative orientations of the two modules are the same in the three copies of CfMan26A-50K in the two crystals characterized.

Sequence similarity searches on the sequence of the β-sheet module alone using protein−protein BLAST (Basic Alignment Search Tool at http://www.ncbi.nlm.nih.gov/BLAST/) did not reveal any database sequences with significant homology. However using the DALI server (*33*), 259 structural homologues with significant *Z*-score (above 2) were identified. The best structural match was to the domain B of unknown function in the glycoside hydrolase glucodextranase (iGDase) from *Arthrobacter globiformis* I42 (*34*), with a *Z*-score of 8.8. All but one of the top fifty structural homologues are classified in the SCOP database (*35*) as possessing an immunoglobulin-like β-sandwich fold. Therefore, we refer to this extra module as an Ig-like module. In the strictly defined immunoglobulin fold, three β-strands

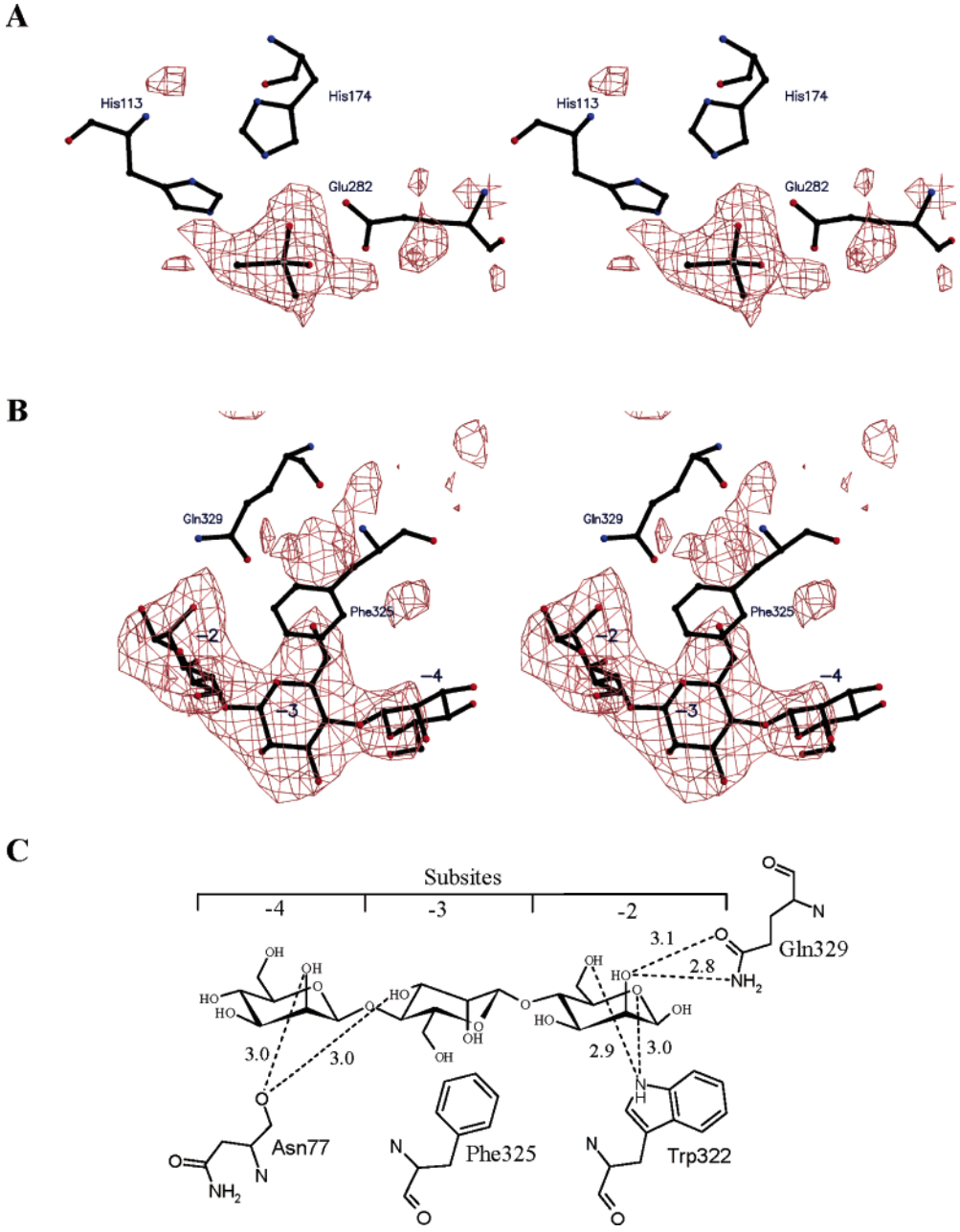

FIGURE 2: (A) Stereoview of the cacodylate ion near the −1 subsite of CfMan26A-50K. (B) Stereoview of mannotriose bound at the −2, −3, and −4 subsites of CfMan26A-50K. Initial $F_o - F_c$ electron density map prior to insertion of the cacodylate ion and mannotriose in the model is shown as a light purple net contoured at 2σ. (C) Schematic representation of the interactions between CfMan26A-50K and mannotriose. Views A and B were prepared with MOLSCRIPT (*44*) and *RASTER3D* (*45*), and representation C was made using Isis/Draw.

(A, B, and E) form one β sheet and four β-strands (D, C, F, and G) form a second sheet (Figure 1B). These two β sheets are closely packed via hydrophobic interactions. The Ig-like module of CfMan26A-50K presents a very similar topology except that the β-strands A, B, E, and D are forming one β sheet while the β-strands C, F, and G form the second β sheet. The electron density was not clear enough to model the residues Gly412−Thr414 in the loop connecting the β-strands C and D, and the residues Thr436−Thr 444 in the long loop connecting β-strands E and F. Even among the top ten DALI hits, several different SCOP superfamilies with Ig-like fold are represented, so that the structural similarity does not give clues as to the function of this module. Several of the *C. fimi* cellulases contain fibronectin type III β-sheet modules of about the same size, but also of unknown functions (*15*).

CBMs in family 9 have Ig-like fold, but the structural representatives of this family are not found among the top 100 structural homologues for CfMan26A-50K. Some CBMs from family 34, also possessing an Ig-like fold, are found among the DALI hits, but evidence for carbohydrate binding has in fact only been put forward for one of the representatives of this family (*36*) (PDB code: 1uh4). Furthermore, no significant binding of CfMan26A-50K to soluble mannan (locust bean gum galactomannan) was observed using affinity electrophoresis, with which binding of the internal mannan-binding module of CfMan26A we previously have shown (*19*). Nor did CfMan26A-50K bind to insoluble mannan from ivory nut, or Avicel cellulose using test tube binding assays as described before (*29*). Thus, the Ig-like module of CfMan26A is unlikely to have a carbohydrate binding function, though it cannot be excluded that it is a vestigial

Table 2: Initial Reaction Products (30 min) of the Hydrolysis of Various Manno-oligosaccharides by CfMan26A-50K

	concentrations of products (mM)				
substrate	M1	M2	M3	M4	M5
M3 10 mM	0.0211	0.0207			
M4 4 mM	0.010	0.009	0.010		
M5 4 mM	0.014	0.025	0.023	0.014	
M6 2 mM	0.0085	0.024	0.012	0.027	0.0052

Table 3: Kinetic Parameters for CfMan26A-50K

substrate	k_{cat} (s^{-1})	K_m (mM)	k_{cat}/K_m (s^{-1} mM^{-1})
M6	77 ± 1.4	0.69 ± 0.03	112
M5	52.42 ± 1.1	1.13 ± 0.06	46.4
M4	11.64 ± 0.55	1.95 ± 0.21	5.98
M3	1.17 ± 0.10	3.1 ± 0.65	0.377

CBM. Another possibility is that it functions as a spacer or linker module between the catalytic domain and the true CBM. Based on the structural results, we propose an updated domain structure for CfMan26A shown in Figure 1D.

Structure of CfMan26A-50K−Mannotriose Complex. The three-dimensional structure of CfMan26A-50K in complex with mannotriose was determined by X-ray crystallography to 2.9 Å resolution. The inspection of the initial electron density map revealed clear density for two mannose moieties of mannotriose spanning the subsites −2 to −3 (Figure 2B) in both molecules in the asymmetric unit. The electron density at the −4 subsite was not as clearly defined relative to the other two subsites, with only half of the sugar ring covered by the electron density. This mannose moiety only interacts with the enzyme through a hydrogen bond (2.8 Å) between the O2 hydroxyl and Asn77 main chain carbonyl oxygen (Figure 2C). Consistently, a higher average temperature factor (47.5 $Å^2$) is observed for the mannose unit at the −4 subsite as compared to mannose units at the −2 and −3 subsites, which were 26.2 $Å^2$ and 28.6 $Å^2$, respectively. At the −2 subsite, the mannose O2 hydroxyl group is hydrogen bonded to NE2 (2.8 Å) and OE1 (3.1 Å) of Gln329, and the O6 and O5 hydroxyls interact via hydrogen bonds (2.9 and 3.0 Å, respectively) with NE1 of Trp322. At the −3 subsite, Phe325 is involved in hydrophobic contact with the mannose moiety, and the O3 hydroxyl is hydrogen bonded (3.0 Å) to the carbonyl oxygen of Asn77. The bound mannotriose did not result in any significant structural changes relative to the native structure.

Hydrolysis of Polysaccharides. The specific activity of CfMan26A-50K using locust bean gum galactomannan as the substrate is 376 kat/mol enzyme and with the more highly substituted guar gum galactomannan 84 kat/mol enzyme. Thus, the enzyme is, in accordance with other β-mannanases (*37*), restricted by the galactose side groups. K_{cat} and K_m for the hydrolysis for locust bean gum galactomannan by CfMan26A-50K were 536 s^{-1} and 2.3 mg/mL, respectively. This K_m value is 2−3 time higher compared to TrMan5A and AnMan5A, and about four times lower than CjMan26A (*11*).

To analyze the end-product formation, ivory nut mannan was extensively hydrolyzed by CfMan26A-50K and the products analyzed with HPLC. The formed products were M2 and M1 in a molar ratio of 0.44:1. These end products are different compared to those observed for some family 5

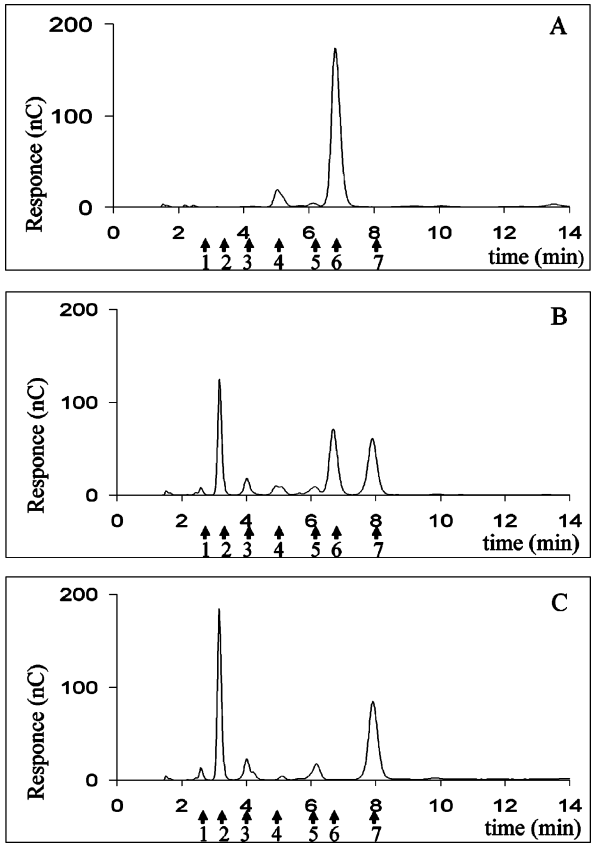

FIGURE 3: The hydrolysis of 1 mM mannopentitol using 20 nM CfMan26A-50K. The chromatograms show the analysis using HPAEC-PAD as described in Experimental Procedures. (A) Hydrolysis mixture without any enzyme added. (B) Hydrolysis after 30 min. (C) Complete hydrolysis after 4 h. The identified peaks are as follows: arrow 1, mannitol; 2, mannobitol; 3, mannose + mannotritol; 4, mannotetritol; 5, mannobiose; 6, mannopentitol; 7, mannotriose. The elution times for M4 and M5 were 10.6 and 13.2 min, respectively.

β-mannanases including TrMan5A for which predominantly M2 and M3 were produced (*20*, *38*).

Hydrolysis of Oligosaccharides. To get a further insight in the degradation process of manno-substrates, CfMan26A-50K was incubated with manno-oligosaccharides. CfMan26A initially (30 min) produced M1, M2, and M3 in the ratio 1:0.9:1 (Table 2) from M4. Interestingly, this is a clear difference compared to CjMan26A which produces almost exclusively M2 from M4 hydrolysis (*11*) and may indicate differences in the organization of the subsites. Furthermore, the hydrolytic release of M1 by CfMan26A-50K appears to be an unusual property among β-mannanases. To elucidate the subsite organization, kinetic analysis of the manno-oligosaccharide hydrolysis was carried out. The Michaelis−Menten enzyme kinetic data is presented in Table 3. Data for M2 could not be obtained because it is extremely slowly hydrolyzed; after 48 h incubation of 10 mM M2 with 3 μM enzyme only 5% of the substrate was hydrolyzed. A decrease of k_{cat}/K_M was observed with decreasing degree of polymerization from M6 to M3. There is nearly a 16-fold and an 8-fold increase of the k_{cat}/K_m values when increasing the degree of polymerization from M3 to M4 and from M4 to M5, respectively. The increase of the degree of polymerization from 5 to 6 (M5 and M6) only gave a 2.4-fold increase in k_{cat}/K_M (Table 3). This means that at least five subsites are required to achieve efficient hydrolysis. In contrast

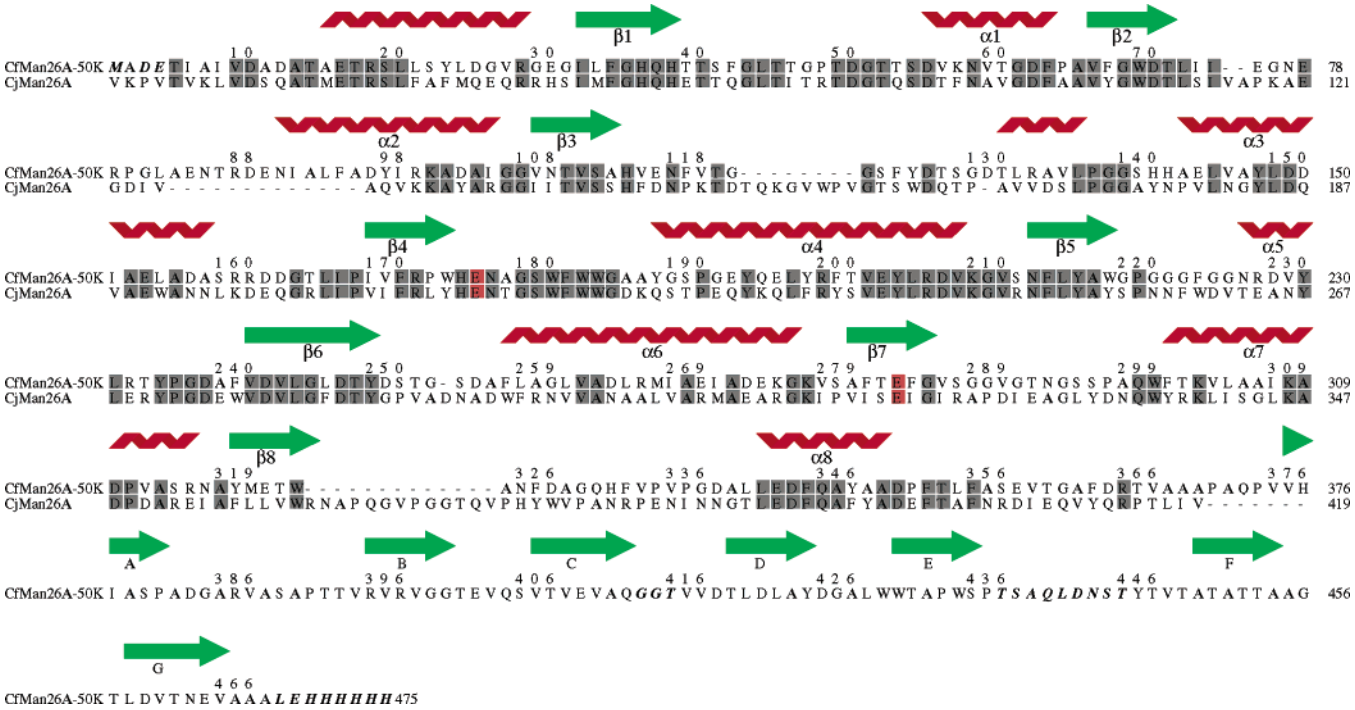

FIGURE 4: Structure-based sequence alignment of the CfMan26A-504q50K and CjMan26A (*PDB code*: 1odz). The β-strands and the α-helices belonging to the $(\beta/\alpha)_8$-barrel of CfMan26A-50K are numbered and colored in green and red, respectively. The β-strands belonging to the β-sheet domain are colored in green and named from letter A to G. Structurally conserved residues (Cα cutoff of 3.8 Å) are shaded. The numbering scheme above the sequence is for CfMan26A-50K. The two catalytic residues are shaded in orange. Glu320 in the CjMan26A structure (PDB code: 1odz) used for comparison is substituted by Gly. The amino acid residues not visible in the crystal structure of CfMan26A-50K are marked in bold and italic. The terminal His residues were introduced to facilitate purification. This figure was prepared with Indonesia (*46*).

CjMan26A only requires four subsites to achieve maximum manno-oligosaccharide hydrolysis efficiency, with an increase of k_{cat}/K_m of less than 2-fold going from M4 hydrolysis to M6 hydrolysis (Hogg et al. (*11*)).

The manno-oligosaccharide hydrolysis strikingly showed that products which add up to the original substrate degree of polymerization are produced in roughly equimolar quantities (i.e. M5 hydrolysis, M1 and M4 (0.014 mM for both) are produced in equimolar quantities, as are M2 (0.025 mM) and M3 (0.023 mM)) (Table 2). These results suggest that CfMan26A-50K does not transglycosylate in contrast to the *Trichoderma reesei* β-1,4-mannanase TrMan5A (*39*, *40*).

Hydrolysis of a Reduced Oligosaccharide. To possibly find out which 5 subsites are the most important, the cleavage pattern of CfMan26A-50K, mannopentitol hydrolysis (1 mM) was carried out. After 30 min the major hydrolysis products released were mannobitol and M3 (0.33 mM) (Figure 3) with minor releases of M2 (0.03 mM). Hence the data suggest that the mannopyranosyl moieties of mannopentitol would preferentially bind from the −3 to the +1 subsite.

Comparison of Substrate Binding and Catalytic Activity in GH26. CjMan26A and CfMan26A are the best characterized GH26 enzymes. A structure-based sequence alignment for the CjMan26A (PDB code: 1odz) and CfMan26A-50K is shown in Figure 4. The two structures superimpose with a 1.1 Å root-mean-square deviation (rmsd), based on 339 C_α atoms.

In the vicinity of the binding subsites −1 and −2 identified in the CjMan26A-Glu320Gly structure (5 Å radius around the bound sugars), the structural alignment showed a high degree of conservation between the CjMan26A and CfMan26A-50K. In CjMan26A, Hogg et al. (*11*) showed by site directed mutagenesis that the two key residues Tyr285 and Trp360 were involved in the substrate binding at the −1 subsite, and these residues are conserved in the CfMan26A-50K structure (Tyr248 and Trp322) (Figure 5). As observed in the CjMan26A-Glu320Gly structure, Tyr248 is hydrogen bonded to the catalytic nucleophile Glu282 in the CfMan26A-50K structure and Trp322 will serve likely as an aromatic platform for the mannopyranose ring at the −1 subsite. Substrate modeling (*11*) in CjMan26A at the +1 subsite showed that Trp217 could serve as hydrophobic platform for the sugar unit at this position, and kinetic analysis revealed that the mutation Trp217Ala decrease significantly the enzyme activity against oligosaccharides. This Trp (Trp180) is conserved in CfMan26A-50K. No major structural differences were observed at the vicinity of the +1 subsite.

Two nonconserved residues Ala323 and Phe325 of CfMan26A-50K are present at the −2 and −3 subsites. The equivalent residues in CjMan26A are Arg361 and Ala363, respectively. In the CjMan26A-Glu320Gly structure in complex with mannobiose (*41*), the O2 and O3 hydroxyl groups of mannose (−2 subsite) are hydrogen bonded to NE (2.8 Å) and NH2 (2.9 Å) of Arg361, respectively (Figure 5). The Arg substitution to Ala in CfMan26A-50K means that it cannot provide these strong interactions at the −2 subsite. On the other hand, Phe325 creates an aromatic platform at the −3 subsite of CfMan26A-50K. By the conjugation of these effects, the relative affinities at the −2 and −3 subsite in CfMan26A-50K are expected to be inverted with respect to CjMan26A.

The kinetic analysis showed that CfMan26A-50K is less active on short manno-oligosaccharides relative to CjMan26A

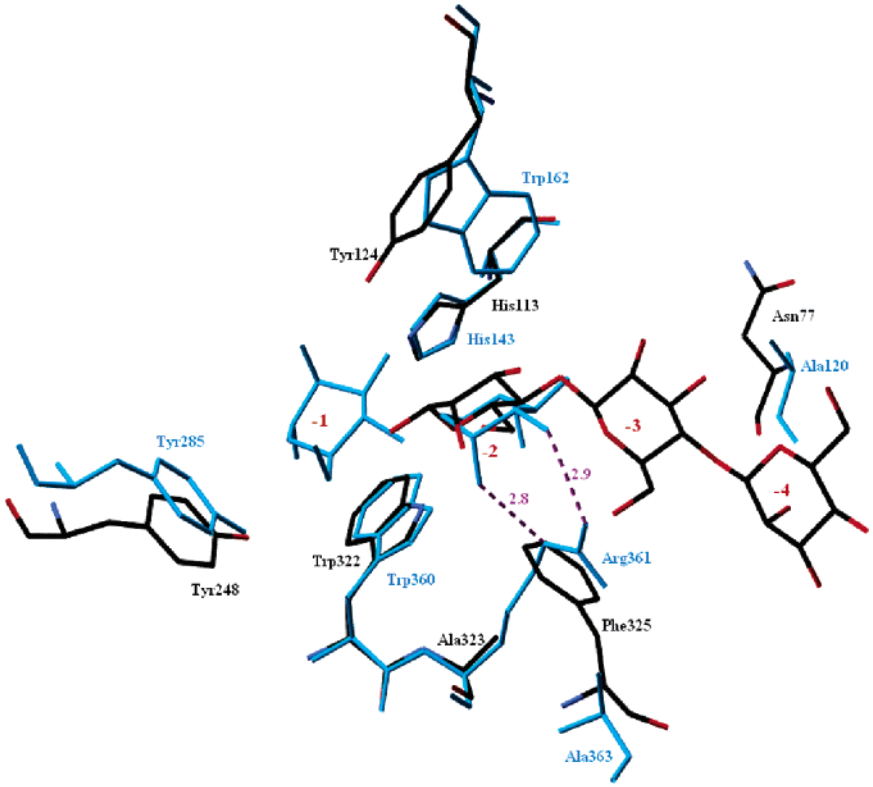

FIGURE 5: Superposition of the CfMan26A-50K in complex with mannotriose and CjMan26A Glu320Gly in complex with mannobiose (PDB code: 1odz) (in light blue) in the vicinity of the nonreducing end binding site. The figure was made with Swiss PDB-viewer (*43*).

and that at least five subsites are required for efficient hydrolysis, as opposed to four. The hydrolysis of mannopentitol by CfMan26A-50K showing the release of M3 and mannobitol as end products (Figure 3) provides evidence for the existence of a strong −3 subsite at the nonreducing end of the substrate binding groove as the crystal structure of CfMan26A-50K in complex with M3 suggests. Considering the products of M4 hydrolysis (Table 2), the available evidence strongly suggests that CfMan26A-50K preferentially hydrolyzes the glycosidic bond at the reducing end of mannotetraose, though the second glycosidic bond could also be hydrolyzed. Lacking a strong −3 subsite, CjMan26A has a more symmetric distribution of products and cannot produce mannose as a major product.

Based on the complex structure, the −4 subsite in CfMan26A probably makes a minor contribution to binding.

Relatively recently, Withers and co-workers applied the "glycosynthase" approach to the family 26 β-1,4-mannanases in order to produce manno-oligosaccharides of defined length (*41*). The approach was tested using the α-mannobiosyl fluoride as sugar donor and numerous *p*-nitrophenyl sugar analogues as acceptors. Their work showed that the CjMan26A inactive catalytic nucleophile mutant Glu320Ser and Glu320Gly had a great ability to function as a "glycosynthase" while the glycosynthesis did not occur with the equivalent CfMan26A-50K nucleophile mutants. Possibly a lack of native transglycosylation capacity, as indicated here, could be a contributing element for the absence of glycosynthase activity. Based on kinetic observations (*42*), Jahn et al. suggested that the −2 subsite of CjMan26A could play an essential role by providing a tighter binding to mannose relative to the CfMan26A-50K allowing the glycosynthesis to occur. The absence in the CfMan26A structure of a residue that can fulfill a similar role to Arg361 of CjMan26A supports this view. The strong −3 subsite in CfMan26A represents an additional factor that could inhibit the "glycosynthase" activity as a nonproductive binding mode of the α-mannobiosyl fluoride to the enzymes is possible.

ACKNOWLEDGMENT

We thank EMBL outstation Hamburg for beam time at station X11, MAXLAB for beam time at I711, and ESRF for beam time at ID-29 and ID23-1. We also thank Flemming Hansen for help with the crystal mounting and Kajsa Sigfridsson, who performed some of the CfMan26A-50K crystallization trials. R.A.J. Warren is thanked for useful discussions.

REFERENCES

1. Lundqvist, J., Teleman, A., Junel, L., Zaachi, G., Dahlman, O., Tjerneld, F., and Stålbrand, H. (2002) Isolation and characterization of galactoglucomannan from Spruce (*Picea abies*), *Carbohydr. Polym. 48*, 29−39.
2. Sjöström, E. (1993) *Wood Chemistry, fundamentals and applications*, 2nd ed., New York, Academic Press Inc., .
3. Koshland, D. E. (1953) Stereochemistry and the mechanism of enzymatic reactions, *Biol. Rev. 28*, 416−436.
4. Henrissat, B., Callebaut, I., Fabrega, S., Lehn, P., Mornon, J.-P., and Davies, G. J. (1995) Conserved catalytic machinery and the prediction of a common fold for several families of glycosyl hydrolases, *Proc. Natl. Acad. Sci. U.S.A. 92*, 7090−7094.
5. Jenkins, J., Lo Leggio, L., Harris, G., and Pickersgill, R. (1995) β-glucosidase, β-galactosidase, family A cellulases, family F xylanases and two barley glucanases form a superfamily of enzymes with 8-fold β/α architecture and with two conserved glutamates near the carboxy-terminal ends of β-strands four and seven, *FEBS Lett. 362*, 281−285.
6. Hilge, M., Gloor, S. M., Rypniewski, W., Sauer, O., Heightman, T. D., Zimmermann, W., Winterhalter, K., and Piontek, K. (1998) High-resolution native and complex structures of thermostable

β-mannanase from *Thermomonospora fusca*-substrate specificity in glycosyl hydrolase family 5, *Structure 6*, 1433−1444.
7. Sabini, E., Schubert, H., Murshudov, G., Wilson, K. S., Siika-Aho, M., and Penttilä, M. (2000) The three-dimensional structure of a *Trichoderma reesei* β-mannanase from glycoside hydrolase family 5, *Acta Crystallogr., Sect. D 56*, 3−13.
8. Bourgault, R., Oakley, A. J., Bewley, J. D., Wilce, M. C. (2005) Three-dimensional structure of (1,4)-β-D-mannan mannanohydrolase from tomato fruit, *Protein Sci. 14*, 1233−1241.
9. Akita, M., Takeda, N., Hirasawa, K., Sakai, H., Kawamoto, M., Yamamoto, M., Grant, W. D., Hatada, Y., Ito, S., and Horikoshi, K. (2004) Crystallization and preliminary X-ray study of alkaline mannanase from an alkaliphilic *Bacillus* isolate, *Acta Crystallogr., Sect. D 60*, 1490−1492.
10. Bolam, D. N., Hughes, N., Virden, R., Lakey, J. H., Hazlewood, G. P., Henrissat, B., Braithwaite, K. L., and Gilbert, H. J. (1996) Mannanase A from *Pseudomonas fluorescens sp. Cellulosa* is a retaining glycosyl hydrolase in which E212 and E230 are the putative catalytic residues, *Biochemistry 35*, 16195−16204.
11. Hogg, D., Woo, E.-J., Bolam, D. N., McKie, V. A., Gilbert, H. J., and Pickersgill, R. W. (2001) Crystal structure of mannanase 26A from *Pseudomonas cellulosa* and analysis of residues involved in substrate binding, *J. Biol. Chem. 276*, 31186−31192.
12. Ducros, V., M.-A., Zechel, D. L., Murshudov, G. N., Gilbert, H. J., Szabó, L., Stoll, D., Withers, S. G., and Davies, G. J. (2002) Substrate distortion by a β-mannanase: Snapshots of the Michaelis and covalent-intermediate complexes suggest a $B_{2,5}$ conformation for the transition state, *Angew. Chem., Int. Ed. 41*, 2824−2827.
13. Stålbrand, H., Saloheimo, A., Vehmaanpera, J., Henrissat, B., Penttilä, M. (1995) Cloning and expression in *Saccharomyces cerevisiae* of a *Trichoderma reesei* β-mannanase gene containing a cellulose binding domain, *Appl. Environ. Microbiol. 61*, 1090−1097.
14. Sunna, A., Gibbs, M. D., and Bergquist, P. L. (2001) Identification of novel β-mannan- and β-glucan-binding modules: evidence for a superfamily of carbohydrate-binding modules, *Biochem. J.* 356, 791−798.
15. Warren, R. A. J. (1996) Microbial hydrolysis of polysaccharides, *Annu. Rev. Microbiol. 50*, 183−212.
16. Couthino, P. M., and Henrissat, B. (1999) Carbohydrate-active enzymes: an integrated database approach, in *Recent advances in carbohydrate bioengineering* (Gilbert, H. J., Davies, G. J., Henrissat, B., and Svensson, B., Eds.), pp 3−12, The Royal Society of Chemistry, Cambridge, England.
17. Boraston, A. B., Bolam, D. N., Gilbert, H. J., and Davies, G. J. (2004) Carbohydrate-binding modules: fine-tuning polysaccharide recognition, *Biochem. J. 382*, 769−781.
18. Stoll, D., Stålbrand, H., and Warren, R. A. J. (1999) Mannan-degrading enzymes from *Cellulomonas fimi*, *Appl. Environ. Microbiol. 65*, 2598−2605.
19. Stoll, D., Boraston, A., Stålbrand, H., McLean, B. W., Kilburn, D. G., and Warren, R. A. J. (2000) Mannanase Man26A from *Cellulomonas fimi* has a mannan-binding module, *FEMS Microbiol. Lett. 183*, 265−269.
20. Stålbrand, H., Siika-aho, M., Tenkanen, M., and Viikari, L. (1993) Purification and characterization of two β-mannanases from *Trichoderma reesei*, *J. Biotechnol. 29*, 229−242.
21. Stura, E. S., Nemerow, G. R., and Wilson, I. A. (1992) Strategies in the crystallization of glycoproteins and protein complexes, *J. Cryst. Growth 122*, 273−285.
22. Cerenius, Y., Ståhl, K., Svensson, A., Ursby, T., Oskarsson, Å., Albertsson, J., and Liljas, A. (2000) The crystallography beamline I711 at MAX II, *J. Synchrotron Radiat. 7*, 203−208.
23. Jancarik, J., and Kim, S. H. (1991) Sparse matrix sampling: a screening method for crystallization of proteins. *J. Appl. Crystallogr. 24*, 409−411.
24. Otwinowski, Z., and Minor, W. (1997) Processing of X-ray diffraction data collected in oscillation mode, *Methods Enzymol. 276*, 307−326.
25. Vagin, A., Teplyakov, A. (1997) MOLREP: An automated program for molecular replacement, *J. Appl. Crystallogr. 30*, 1022−1025.
26. Brünger, A. T. (1992) Free *R* value: a novel statistical quantity for assessing the accuracy of crystal structures, *Nature 355*, 472−475.
27. Brünger, A. T., Adams, P. D., Clore, G. M., DeLano, W. L., Gros, P. Grosse-Kunstleve, R. W., Jiang, J. S., Kuszewski, J., Nilges, M., Pannu, N. S., Read, R. J., Rice, L. M., Simonsen, T., and Warren, G. L. (1998) Crystallography & NMR system: a new software suite for macromolecular structure determination, *Acta Crystallogr., Sect. D 54*, 905−921.
28. Jones, T. A., Zou, J. Y., Cowan, S. W., and Kjeldgaard, M. (1991) Improved methods for building protein models in electron density maps and location of the errors in these models, *Acta Crystallogr., Sect. A* 47, 110−119.
29. Hägglund, P., Eriksson, T., Collén, A., Nerinckx, W., Claeyssens, M., and Stålbrand, H. (2003) A cellulose-binding module of the *Trichoderma reesei* beta-mannanase Man5A increases the mannan-hydrolysis of complex substrates, *J. Biotechnol. 101*, 37−48.
30. Schou, C., Rasmussen, G., Kaltoft, M. B., Henrissat, B., and Schulein, M. (1993) Stereochemistry, specificity and kinetics of the hydrolysis of reduced cellodextrins by nine cellulases, *Eur. J. Biochem. 217*, 947−953.
31. Bray, M. R., and Clarke, A. J. (1992) Action pattern of xylo-oligosaccharide hydrolysis by *Schizophyllum commune* xylanase A, *Eur. J. Biochem. 204*, 191−196.
32. Sakon, J., Irwin, D., Wilson, D. B., and Karplus, P. A. (1997) Structure and mechanism of endo/exocellulase E4 from *Thermomonospora fusca*, *Nat. Struct. Biol. 10*, 810−818.
33. Holm, L., and Sander, C. (1993) Protein structure comparison by alignment of distance matrices, *J. Mol. Biol. 233*, 123−138.
34. Mizuno, M., Tonozuka, T., Suzuki, S., Uotsu-Tomita, R., Kamitori, S., Nishikawa, A., and Sakano, Y. (2004) Structural insights into substrate specificity and function of glucodextranase, *J. Biol. Chem. 279*, 10575−10583.
35. Murzin, A. G., Brenner, S. E., Hubbard, T., and Chothia, C. (1995) SCOP: a structural classification of proteins database for the investigation of sequences and structures, *J. Mol. Biol. 247*, 536−540.
36. Abe, A., Tonozuka, T., Sakano, Y., and Kamitori, S. (2004) Complex structures of *Thermoactinomyces* vulgaris R-47 alpha-amylase 1 with malto-oligosaccharides demonstrate the role of domain N acting as a starch-binding domain, *J. Mol. Biol. 335*, 811−822.
37. Stålbrand, H. (2003) Enzymology of endo-1,4-β-mannanases, in *Handbook of food enzymology* (Whitaker, J. R., Voragen, A. G. J., and Wong, D. S. W., Eds.), pp 961−969, Marcel Dekker, Inc., New York.
38. Ademark, P., Varga, A., Medve, J., Harjunpää, V., Drakenberg, T., Tjerneld, F., and Stålbrand, H. (1998) Softwood hemicellulose-degrading enzymes from *Aspergillus niger*: purification and properties of a β-mannanase, *J. Biotechnol. 63*, 199−210.
39. Harjunpää, V., Teleman, A., Siika-aho, M., and Drakenberg, T. (1995) Kinetic and stereochemical studies of manno-oligosaccharide hydrolysis catalysed by β-mannanases from *Trichoderma reesei*, *Eur. J. Biochem. 234*, 278−283.
40. Harjunpää, V., Helin, J., Koivula, A., Siika-aho, M., and Drakenberg, T. (1999) A comparative study of two retaining enzymes of *Trichoderma reesei*: transglycosylation of oligosaccharides catalyzed by the cellobiohydrolase I, Cel7A, and the β-mannanase, Man5A, *FEBS Lett. 443*, 149−153.
41. Jahn, M., Stoll, D., Warren, R. A. J., Szabó, L., Singh, P., Gilbert, H. J., Ducros, V. M.-A., Davies, G. J., and Withers, S. G. (2003) Expansion of the glycosynthase repertoire to produce defined manno-oligosaccharides, *Chem. Commun. 12*, 1327−1329.
42. Hogg, D., Pell, G., Dupree, P., Goubet, F., Martìn-Orùe, S. M., Armand, S., and Gilbert, H. J. (2003) The modular architecture of *Cellvibrio japonicus* mannanases in glycoside hydrolase families 5 and 26 points to differences in their role in mannan degradation, *Biochem. J. 371*, 1027−1043.
43. Guex, N., and Peitsch, M. C. (1997) SWISS-MODEL and the Swiss-Pdb viewer: An environment for comparative protein modelling, *Electrophoresis 18*, 2714−2723.
44. Kraulis, P. J. (1991) MOLSCRIPT: A program to produce both detailed and schematic plots of protein structures, *J. Appl. Crystallogr. 24*, 949−950.
45. Merritt, E. A., and Bacon, D. J. (1997) *RASTER3D* version 2: photorealistic molecular graphics. *Methods Enzymol. 277*, 505−524.
46. Madsen, D., Johansson, P., Johansson, N., Arent, S., Harris, M. R., and Kleywegt, G. J. INDONESIA: An integrated workbench for sequence and structure alignment and analysis, manuscript submitted.
47. Laskowski, R. A., MacArthur, M. W., Moss, D. S., and Thornton, J. M. (1993) PROCHECK: A program to check the stereochemical quality of protein structures, *J. Appl. Crystallogr. 26*, 283−291.

BI050779V